XX Congreso de Ecuaciones Diferenciales y Aplicaciones
X Congreso de Matemática Aplicada
Sevilla, 24-28 septiembre 2007
(pp. 1–8)

The dynamics around the collinear point L_3 of the RTBP

E. Barrabés[1], J.M. Mondelo[2], M. Ollé[3]

[1] *Dept. Informàtica i Matemàtica Aplicada, Universitat de Girona, 17071, Girona, Spain. E-mail:* barrabes@ima.udg.edu.
[2] *Dept. de Matemàtiques, Universitat Autònoma de Barcelona, Campus de Bellaterra, Ed. C, 08193-Bellaterra (Barcelona), Spain. E-mail:* jmm@mat.uab.es.
[3] *Dept. de Matemàtica Aplicada I, ETSEIB, Universitat Politècnica de Catalunya, Diagonal 647, 08028 Barcelona, Spain. E-mail:* merce.olle@upc.edu.

Palabras clave: RTBP, collinear points, periodic orbits, homoclinic orbits

Resumen

We consider the Restricted Three Body Problem (RTBP), and we restrict our attention to the equilibrium point L_3. Our aim is centered in the description, as global as possible, of the dynamics around this equilibrium point. In this communication, we initially consider small values of μ, for which homoclinic connections to the equilibrium point L_3 are horseshoe-shaped, and then, other values of μ are considered. We compute the objects in the center manifold of L_3, including the invariant manifolds associated with them. They are computed by purely numerical procedures, in order to avoid the convergence restrictions of the semi-analytical ones (typically used around L_1 or L_2). We deal with homoclinic connections of periodic orbits and develop some numerical tools in order to compute them. These tools can be extended to compute also homoclinic connections to invariant tori.

1. Introduction

Let us consider the circular restricted three-body problem (RTBP) where two bodies (called primaries) describe circular orbits around their common center of mass, and a third body of infinitesimal mass moves under the gravitational effect of the primaries but having negligible effect on their motion. With suitable units, we can assume that the primaries have masses $1-\mu$ and μ, $\mu \in (0, 1/2]$, that the period of their motions is 2π and that their distance is the unit. Let $\mathbf{r} = (x, y, z)$ be the coordinates of the third body and $\mathbf{p} = (p_x, p_y, p_z)$ the corresponding momenta in a rotating reference system where

the primaries are fixed at $(\mu, 0, 0)$ and $(\mu - 1, 0, 0)$. Then, the Hamiltonian governing the motion of the infinitesimal particle is given by

$$\mathcal{H} = \frac{1}{2}(p_x^2 + p_y^2 + p_z^2) - xp_y + yp_x - \frac{1-\mu}{r_1} - \frac{\mu}{r_2}, \tag{1}$$

where $r_1 = \sqrt{(x-\mu)^2 + y^2 + z^2}$ and $r_2 = \sqrt{(x-\mu+1)^2 + y^2 + z^2}$ (see, for example [8]). The value of the Hamiltonian on each orbit will be referred to as the energy of the orbit and its relation with the Jacobi integral is given by $\mathcal{C} = -2\mathcal{H} + \mu(1-\mu)$. Furthermore, the equations of the problem satisfy the symmetries

$$\begin{array}{rcl} (t, x, y, z, p_x, p_y, p_z) & \longrightarrow & (-t, x, -y, z, -p_x, p_y, -p_z), \\ (t, x, y, z, p_x, p_y, p_z) & \longrightarrow & (-t, x, -y, -z, -p_x, p_y, p_z). \end{array} \tag{2}$$

The RTBP has five equilibrium points: the collinear points, L_1, L_2 and L_3, and the equilateral ones, L_4 and L_5. We will consider L_1 located between the two primaries, L_2 located such that the small primary is between L_1 and L_2, and L_3 such that the big primary is between L_1 and L_3. We denote by $\mathcal{C}_i$ and $\mathcal{H}_i$ the value of the Jacobi constant and the energy at the equilibrium point L_i, $i = 1, \ldots, 5$. It is well known that $3 = C_4 = C_5 < C_3 \leq C_2 < C_1$, and $C_3 = C_2$ for $\mu = 1/2$.

In this communication, we focus our attention on the dynamics of the RTBP around the equilibrium point L_3. The dynamics around the collinear points have been studied by several authors using different techniques and approaches (see, for example, [3], [4], [5], [6] and the references therein). It is well known that the linear behaviour of the three points is of type center×center×saddle. In spite of this, there is a strong difference between L_i, $i = 1, 2$, and L_3: while the first two points are strongly affected by both primaries, the effect of the small primary on L_3 is almost negligible. Furthermore, in the case of L_1 and L_2, the invariant manifolds can be computed in series expansion by semi-analytical procedures as the ones based in Lindstedt-Poincaré method or reduction to the center manifold (see [7]). These methods produce expansions of the manifolds up to an arbitrary order, which give initial conditions on the manifolds up to a high degree of accuracy. However, these methods are not suitable for the neighbourhood of L_3 due to the small range of values of the energy for which the truncated series are valid.

We explore numerically the existence and organization of invariant objects around L_3, as well as the existence of homoclinic orbits. We start dealing with the invariant manifolds of the equilibrium point L_3 and then with the families of planar Lyapunov periodic orbits (LPO) that are born at L_3. Then, the invariant manifolds associated with LPO are considered. We develop numerical methods in order to compute, at the same time, both a periodic orbit and an homoclinic connection to it. The explorations are done for $\mu \in [10^{-4}, 0.03]$, which contains the Earth-Moon value, $\mu_{EM} = 0.01215058560962404$ and the Sun-Jupiter value, $\mu_{SJ} = 9.53875 \times 10^{-4}$. Finally, we generalize the methods used in order to find homoclinic connections to invariant tori.

2. Linear behaviour around L_3 and homoclinic phenomena

It is well known that the linear behaviour of the equilibrium points is of type center × center × saddle and that two families of periodic orbits are born at them: the planar and

vertical Lyapunov orbits. In the case of the planar Lyapunov orbits (see, for instance, [4]), and for values of the energy less than the first vertical bifurcation orbit (corresponding to the value at which the family of Halo orbits is born), the orbits have central and hyperbolic parts. For a fixed value of the energy, the corresponding Lyapunov orbit has stable and unstable invariant manifolds and there exists a (cantorian) family of invariant tori connecting the planar orbit with the vertical one with the same energy. Each of these tori inherits the hyperbolic behaviour of the backbone periodic orbits.

Let X be one of the invariant objects around L_3. We denote by $W^u(X)$ the unstable manifold and $W^s(X)$ the stable one (or simply W^u and W^s). In the case of a collinear equilibrium point, the invariant manifolds have dimension 1 and contain planar orbits that tend (backwards or forwards in time) to the equilibrium point. For each manifold, $W^{u/s}_+(L_i)$ denotes the branch corresponding to the eigenvector that points to the upper half plane $\{y > 0\}$ and by $W^{u/s}_-(L_i)$ the branch corresponding to the eigenvector pointing to the lower half plane $\{y < 0\}$. This notation can be extended for the branches of the invariant manifolds of a periodic orbit or an invariant torus: $W^{u/s}_+$ (respectively $W^{u/s}_-$) denotes the branch that enters into the upper space $\{y > 0\}$ (resp. lower space $\{y < 0\}$) after leaving forward (resp. backward) in time a neighbourhood of the invariant object. We observe that the symmetries given by (2) map orbits on W^u_- to W^s_+ and vice versa.

We are interested in homoclinic connections to an invariant object X, which are solutions of the RTBP such that tend to X forward and backward in time. Such solutions belong to the stable and unstable manifolds associated with X, this is, to the intersection $W^u \cap W^s$. In order to compute homoclinic orbits, we fix a Poincaré section Σ and we look for elements of $\left(W^u \cap \Sigma^j\right) \cap \left(W^s \cap \Sigma^k\right)$, where $W^{u/s} \cap \Sigma^m$ denotes the m-th intersection of the invariant manifold with Σ. Depending on the branches that are involved we look for the following kinds of homoclinic connections:

- connection of type $(-j, -k)$, which takes place when $\left(W^u_- \cap \Sigma^j\right) \cap \left(W^s_- \cap \Sigma^k\right) \neq \emptyset$. Similarly, a connection of type $(+j, +k)$ can be defined. Observe that, if there exists a connection of type $(-j, -k)$, then it is a non-symmetric orbit and the symmetric orbit is a connection of type $(+j, +k)$.

- connection of type $(-j, +k)$, which takes place when $\left(W^u_- \cap \Sigma^j\right) \cap \left(W^s_+ \cap \Sigma^k\right) \neq \emptyset$. Similarly, a connection of type $(+j, -k)$ can be defined. If there exist symmetric connections, they must be of one of these types.

3. Homoclinic connections to L_3

In this Section, we look for values of μ for which there exists an homoclinic connection to L_3. Font, in [2], proved that there exists an infinite sequence of μ tending to zero, such that there exists an homoclinic connection to L_3 for each one of these values. These connections are all symmetric. In [1], the behaviour of the invariant manifolds of L_3 as μ varies and its relation with horseshoe orbits are described and a procedure to compute symmetric homoclinic connections to L_3 using the symmetry of the orbits is given. Here we want to generalize that procedure in order, to find, if they exist, non symmetric connections as well.

We consider in this section $\Sigma = \{x = \mu - 1/2\}$. We start with an initial condition on the linear approximation of the invariant manifold, and we follow the flow of the RTBP until the corresponding intersection with Σ. As the invariant manifolds are 1-dimensional, $W_{\pm}^{u/s} \cap \Sigma^m$ consists of one point $\mathbf{z}^{u/s}(\mu)$, so we look for values of μ such that $\mathbf{z}^u(\mu) = \mathbf{z}^s(\mu)$. We consider the values of $\mu \in [10^{-4}, 0.03]$, which contains the cases of Sun-Jupiter and Earth-Moon problems.

Concerning homoclinic connections of type $(-j, -k)$, we explore the cases $(-1, -2)$, $(-2, -3)$ and $(-3, -4)$ and we do not observe numerical evidence of non-symmetric homoclinic connections.

In the case of an equilibrium point, all homoclinic connections of type $(-j, +k)$ or $(+j, -k)$ are symmetric (which is not true in the case of periodic orbits or invariant tori). We explore the cases $j = 2, k = 3$ and $j = 2, k = 5$ and $j = 4, k = 5$. We find homoclinic connections in all of them, in particular, all the symmetric homoclinic orbits described in [1]. In Figure 1, two different homoclinic orbits to L_3 for different values of μ are shown.

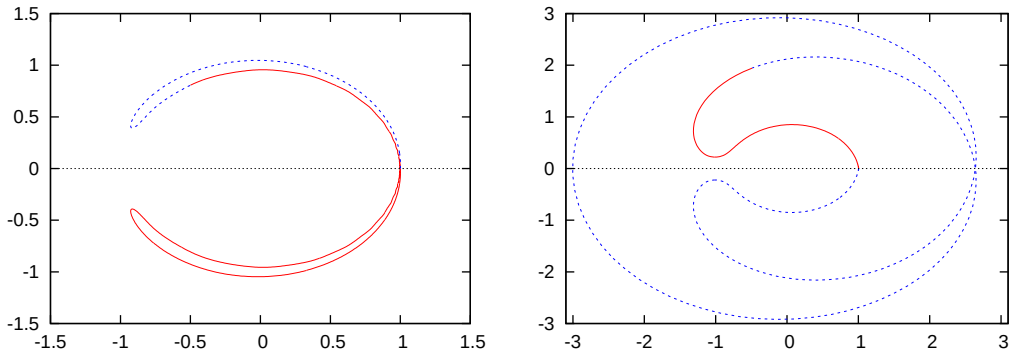

Figura 1: Homoclinic orbits to L_3 of type $(-3, 2)$ for $\mu = 0.0010015432$ (left) and $(+2, -5)$ for $\mu = 0.012143988024852$ (right). (W^u in continuous red line, W^s in dashed blue line)

4. Homoclinic connections to Lyapunov orbits

In this section we deal with the family of planar Lyapunov periodic orbits (LPO) around L_3 and their homoclinic orbits. For values of the energy $\mathcal{H}$ close to $\mathcal{H}_3$, the LPO inherit the behaviour of the equilibrium point, so the associated invariant manifolds have a shape similar as the invariant manifolds of L_3. Fixed a planar Lyapunov orbit X, we consider the different branches of each invariant manifold $W^{u/s}(X)$, and we look for their intersections with the section $\Sigma = \{x = \mu - 1/2\}$. The invariant manifolds are 2-dimensional objects that can be viewed as tubes in the phase space. It can be expected that the first crossings of each $W_{\pm}^{u/s}(X)$ with Σ will be like S^1 curves, so one way to compute the homoclinic connections is to look for the intersections of these curves (see Figure 2). However, this procedure presents some problems when the energy or μ increases due to the presence of multiple loops that make difficult to compute 'exactly' the m-th crossing with a section (see Figure 5). In this case, we use a different approach in order to find a specific homoclinic orbit without computing the whole curve $W_{\pm}^{u/s}(X) \cap \Sigma^m$.

Next, we describe slightly the methods used.

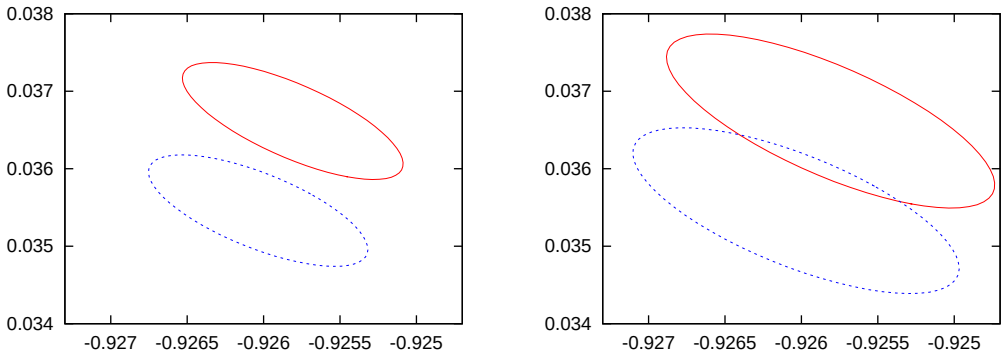

Figura 2: $W^u_- \cap \Sigma^1$ and $W^s_- \cap \Sigma^2$ curves in the (y, y') plane ($y' = p_y - x$) for two planar LPO around L_3 of energy $\mathcal{H} = -1.500476742438758$ (left) and $\mathcal{H} = -1.500476517438758$ (right). ($\mu = \mu_{SJ}$ and $\Sigma = \{x = \mu - 1/2\}$)

1. *Intersection of the invariant manifolds with a defined section.*
   Fixed X a periodic orbit, a simple method consists of taking, for each point of the orbit, the linear approximation of the invariant manifold, and follow the flow (forward or backward, depending on the manifold) by numerical integration until the desired intersection with Σ. This method has problems when the orbit on the manifold has loops. In this case, we use a global parametrization of an invariant manifold in order to obtain a parametrization of the curve $W^{u/s}_\pm(X) \cap \Sigma^m$. In Figures 2 and 5 the intersections of the invariant manifolds with different sections ($\Sigma = \{x = \mu - 1/2\}$ and $\Sigma' = \{y = 0\}$) for different LPO are shown.

   Once we have the two curves, obtained from the intersection of each invariant manifold and Σ, the homoclinic orbits can be computed as the intersection of both curves. As we have them as a union of polygons, we can check for intersections between segments and then refine the process.

2. *Computation of a homoclinic of a periodic orbit: matching of manifolds on a section.*
   The idea is to compute directly an homoclinic orbit without computing the whole intersection of an invariant manifold with a section. In order to do this, we look for two orbits, each one in a different invariant manifold, such that match at their corresponding intersection with Σ. We remark that in order to obtain robust results this method is implemented by using a multiple shooting strategy.

   As we have said before, as the energy increases, so do the loops, which is a problem if the number of intersections with Σ is fixed. In order to avoid counting the number of intersections when computing an homoclinic orbit, we introduce in the equations as an unknown quantity the time to reach Σ. Finally, if we want to implement a continuation method it is necessary to vary the periodic orbit. Thus we compute, at each step, a periodic orbit and an homoclinic connection to it.

Let us show some of the results obtained.

We consider the mass parameter $\mu_{SJ} = 9.53875 \times 10^{-4}$. We start looking for homoclinic orbits of type $(-1, -2)$. We consider the section $\Sigma = \{x = \mu - 1/2\}$ and compute the curves

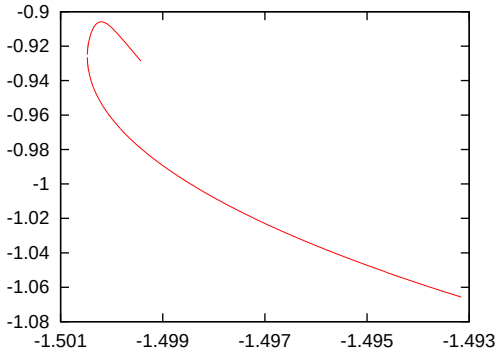

Figura 3: Characteristic curve $(\mathcal{H}, y)$ of a family of homoclinic orbits to Lyapunov orbits for $\mu = \mu_{SJ}$.

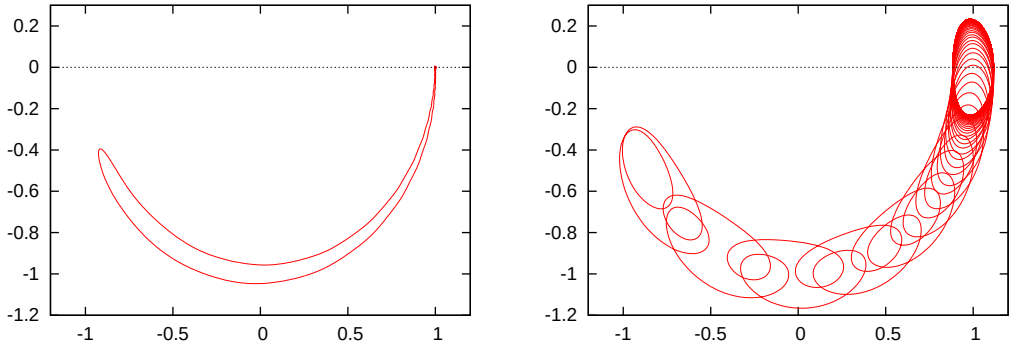

Figura 4: Non symmetric homoclinic orbits for $\mu = \mu_{SJ}$ $\mathcal{H} = -1.5004762674387578125$ (left) and $\mathcal{H} = -1.4935767674387578125$ (right).

$W^u_- \cap \Sigma^1$ and $W^s_- \cap \Sigma^2$, which can be represented in the (y, y') plane ($y' = p_y - x$). Recall that there is no homoclinic connection to L_3 of this type. Then, for values of $\mathcal{H}$ slightly bigger than H_3, no homoclinic orbits of this type are expected, and the curves do not intersect (see Figure 2 left). But as we increase $\mathcal{H}$, first the curves become tangent at one point –so there is one homoclinic orbit–, and then intersect at two points, giving rise to two homoclinic orbits (see Figure 2 right).

Then, given a homoclinic orbit, we follow the family it belongs to, predicting a new orbit using the tangent vector to the curve that represents the family of homoclinic orbits. As the energy increases, the number of loops increases as well, so although we start the family with a homoclinic orbit of type $(-1, -2)$, it is possible to find other homoclinic orbits with a different number of intersections with Σ in the same family. In Figure 3 the characteristic curve of a family of homoclinic orbits in the $(\mathcal{H}, y)$ plane is shown, being y the second coordinate of the matching point of the invariant manifolds at Σ. In Figure 4 two non symmetric homoclinic orbits are shown.

All of the above homoclinic connections are non-symmetric orbits. In order to find symmetric homoclinic orbits, we consider the $(-1, +4)$ case. We start considering a LPO with $\mathcal{H} = -1.500476742438758$, for which there no exists connections of type $(-1, -2)$, and

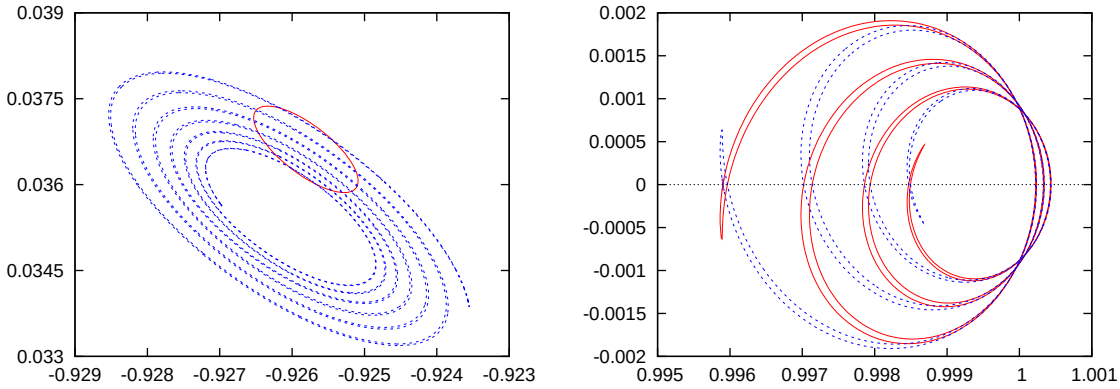

Figura 5: Intersection of the invariant manifolds of a periodic orbit for $\mu = \mu_{SJ}$ and $\mathcal{H} = -1.500476742438758$ with two different sections: $W^u_- \cap \Sigma^1$ and $W^s_+ \cap \Sigma^4$ curves in the (y, y') plane (left), $W^u_- \cap \Sigma'$ and $W^s_+ \cap \Sigma'$ curves in the (x, x') plane (right).

we compute $W^u_- \cap \Sigma^1$ and $W^s_+ \cap \Sigma^4$. The curves obtained, represented in the (y, y')-plane, are shown in Figure 5, left, where the effect of the loops can be observed. In this case we obtain 28 intersection points, that is, 28 homoclinic orbits which contain symmetric and nonsymmetric homoclinic orbits. In order to identify the symmetric orbits, sometimes it is more convenient to deal with the section $\Sigma' = \{y = 0\}$, because the symmetric orbits correspond to the points on the curves with $x' = 0$. In Figure 5, right, $W^u_- \cap \Sigma'$ and $W^s_+ \cap \Sigma'$, for the same periodic orbit as before, are shown, where, 14 homoclinic symmetric orbits can be identified.

5. Homoclinic connections to invariant tori

Consider a level of energy smaller than the first bifurcation of the family of planar Lyapunov orbits. The family of invariant tori of this energy level connecting the planar and the vertical Lyapunov orbits inherit the hyperbolic behaviour of the periodic orbits. Thus, for each invariant torus, we can consider the 3-dimensional invariant manifolds associated to them and we can look for homoclinic connections considering again the intersection of each branch of the invariant manifolds with a given section. The method of computing homoclinic orbits looking for two specific orbits in each invariant manifold and doing section matching can be generalized to invariant tori. In Figure 6 two different homoclinic orbits for the same invariant torus are shown.

Acknowledgments

E. Barrabés and J.M. Mondelo are partially supported by the MCyT/FEDER grants BFM2003-09504-C02-01 and MTM2006-05849/Consolider. J.M. Mondelo is also supported by the MCyT/FEDER grant MTM2005-02139. M. Ollé is partially supported by the MCyT/FEDER grant MTM2006-00478.

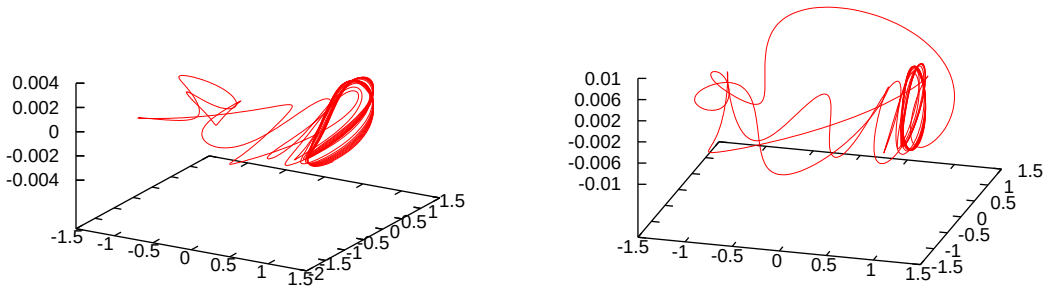

Figura 6: Homoclinic connections to an invariant tori for $\mu = \mu_{SJ}$ and $\mathcal{H} = -1.46$ (left) and $\mathcal{H} = -1.5$ (right).

Referencias

[1] Esther Barrabés and Mercè Ollé. Invariant manifolds of l_3 and horseshoe motion in the restricted three-body problem. *Nonlinearity*, 19:2065–2089, 2006.

[2] J. Font. *The role of homoclinic and heteroclinic orbits in two-degrees of freedom Hamiltonian systems*. PhD thesis, University of Barcelona, 1999.

[3] G. Gómez, A. Jorba, J Masdemont, and C. Simó. Study of poincaré maps for orbits near lagrangian points. Final report, ESOC contract 971191/D/IM(SC), 1993.

[4] G. Gómez and J. M. Mondelo. The dynamics around the collinear equilibrium points of the RTBP. *Phys. D*, 157(4):283–321, 2001.

[5] Àngel Jorba and Josep Masdemont. Dynamics in the center manifold of the collinear points of the restricted three body problem. *Phys. D*, 132(1-2):189–213, 1999.

[6] W. S. Koon, M. W. Lo, J. E. Marsden, and S. D. Ross. Heteroclinic connections between periodic orbits and resonance transitions in celestial mechanics. *Chaos*, 10(2):427–469, 200.

[7] J. Masdemont. High-order expansions of invariant manifolds of libration point orbits with applications to mission design. *Dynamical Systems: An International Journal*, 20(1):59–113, March 2005.

[8] Kenneth R. Meyer and Glen R. Hall. *Introduction to Hamiltonian dynamical systems and the N-body problem*, volume 90 of *Applied Mathematical Sciences*. Springer-Verlag, New York, 1992.